Original Research

DERMATOLOGY

Untargeted serum metabolomics reveals metabolic signatures distinguishing basal cell carcinoma risk groups: an exploratory analysis

Amalia Moisoiu[1,2], Tudor Moisoiu[3], Corina Bocșa[4], Carmen Socaciu[5], Daniela Fodor[2,6]

1) Department of Dermatology, County Emergency Clinical Hospital, Cluj-Napoca, Romania

2) Iuliu Hatieganu University of Medicine and Pharmacy, Napoca, Cluj-Napoca, Romania

3) Clinical Institute of Urology and Renal Transplantation, Cluj-Napoca, Romania

4) Interservisan Medical-Surgical Center, Cluj-Napoca, Romania

5) Center for Applied Biotechnology Biodiatech, S.C. Proplanta S.R.L., Cluj-Napoca, Romania

6) 2nd Internal Medicine Department, Iuliu Hatieganu University of Medicine and Pharmacy Cluj-Napoca, Cluj-Napoca, Romania

Abstract

Background and aim. Basal cell carcinoma (BCC) is the most common skin cancer, yet reliable non-invasive markers for distinguishing low-risk (LR) from high-risk (HR) lesions are still lacking. Serum metabolomics provides a promising approach for capturing systemic biochemical changes associated with tumor behavior. In this study, we conducted untargeted serum metabolomic profiling using high-performance liquid chromatography coupled with mass spectrometry in 48 patients with histologically confirmed BCC.

Methods. The cohort included 38 HR and 10 LR lesions. After quality filtering, 99 polar and 54 lipophilic metabolites were retained for analysis. Using a significance threshold of $P < 0.01$ and absolute fold change > 1.2, 10 metabolites differed between HR and LR BCC.

Results. Principal component analysis showed partial separation between the two groups driven by metabolites including dihydroxybutyric acid, glucosylsphingosine, androsterone, and several lysophosphatidylcholines. A linear discriminant model based on the first 4 principal components achieved an AUC of 0.88, corresponding to a sensitivity of 89% and a specificity of 40% for identifying HR lesions. Enrichment analysis revealed representation of multiple chemical classes, including carboxylic acids, steroids, glycerophospholipids, indoles, diazines, and organooxygen compounds. Several metabolites varied significantly by anatomical location and tumor size, while histologic subtype showed no meaningful influence.

Conclusions. These findings provide initial evidence that serum metabolomics can detect metabolic differences between LR and HR BCC and may serve as a basis for developing non-invasive biomarkers to improve BCC risk stratification

Keywords: metabolomics, skin cancer, cutaneous malignancies, basal cell carcinoma

DOI: 10.15386/mpr-2961

Manuscript received: 21.12.2025
Received in revised form: 27.01.2026
Accepted: 29.01.2026

Address for correspondence:
Daniela Fodor
dfodor@ymail.com

Background and aims

Basal cell carcinoma (BCC) is the most frequent cutaneous malignancy, accounting for 75% of newly diagnosed skin cancers. Its incidence is currently rising by 1–3% annually in the United States and Europe [1].

Despite a low mortality rate (<1%) [2], the tumor's predilection for the head and neck mandates that treatment goals prioritize not only cure but also the maximal preservation of function and cosmetics [3,4]. Consequently, both US and European guidelines propose a risk stratification approach regarding recurrence [1,5]. This assessment relies on clinical, dermatoscopic, and histological evaluations prior to therapeutic decision-making. Non-invasive options, such as cryotherapy, curettage, electrodessication, photodynamic therapy, or topical treatments with imiquimod or 5-fluorouracil, are generally reserved for low risk (LR) lesions. Conversely, high

risk (HR) lesions require surgical excision with 4–5 mm margins or Mohs micrographic surgery.

Risk classification of BCC remains challenging because aggressive histologic subtypes can present with deceptively benign clinical features, biopsy sampling may miss focal areas of HR pathology, and both dermatoscopy and imaging have inherent diagnostic limitations. Moreover, current classification systems are not fully harmonized, and significant interobserver variability across clinical, dermatoscopic, and histopathologic assessments further complicates accurate risk stratification [6]. Patient-specific factors such as immunosuppression, prior treatments, and lesion recurrence add an additional layer of complexity [7]. No molecular biomarker is currently available to reliably assess recurrence risk or disease aggressiveness.

These diagnostic constraints highlight the need for objective, molecularly driven markers to refine existing risk-stratification approaches. In this context, serum metabolomics offers a non-invasive window into tumor-related biochemical alterations and represents a promising strategy to uncover molecular signatures associated with BCC recurrence risk [8].

However, the evidence characterizing the blood metabolomic profile of BCC remains scarce. Indeed, most serum metabolomics studies to date have focused on melanoma [9–13], and the current metabolomics literature in BCC is limited and relies largely on indirect, experimental, or tissue-based approaches. One recent study employed MALDI mass spectrometry imaging combined with machine learning and reported high diagnostic accuracy for BCC; however, the analysis was conducted on a small number of experimentally induced tumors in a murine model and was restricted to tissue-level metabolic profiling, thereby limiting its translational relevance for non-invasive risk stratification in humans [14].

Similarly, available human studies remain constrained by tissue-based designs and small sample sizes. Electroporation-based biopsy coupled with high-throughput lipidomics has been shown to differentiate BCC from healthy skin and squamous cell carcinoma, but this approach requires direct tissue sampling, includes a limited number of patients, and does not assess circulating metabolites, precluding its application to non-invasive risk stratification or systemic biomarker discovery [15].

Large-scale human data addressing circulating metabolites in BCC are also limited by indirect inference frameworks. A recent Mendelian randomization study explored genetic associations between circulating metabolites, immune parameters, and skin cancer risk; however, the analysis relied on genetically inferred metabolite traits derived from GWAS data rather than direct experimental metabolomic profiling of patient samples, and it did not enable discrimination between HR and LR BCC lesions at the individual level [16].

Collectively, these studies highlight the paucity of data directly addressing serum metabolomic differences between clinically defined LR and HR BCC. This gap underscores the need for exploratory, proof-of-concept investigations based on direct serum metabolomic profiling to evaluate whether circulating metabolic signatures reflect BCC risk stratification. To address this gap, we conducted an untargeted analysis using high-performance liquid chromatography coupled with mass spectrometry (LC-MS).

Our study pursued two main objectives. First, we aimed to determine whether LR and HR BCC exhibit distinct circulating metabolic profiles. Second, once metabolic differences were identified, we examined which factors were most closely associated with these differences, including tumor size, anatomical site and histologic subtype.

By uncovering serum metabolomic profiles that differentiate LR and HR BCC, this exploratory study provides objective preliminary insights. These findings lay the groundwork for more accurate risk stratification and may ultimately support more individualized treatment decisions.

Methods

Consecutive participants were recruited from the Department of Dermatology at the County Emergency Clinical Hospital Cluj-Napoca in Cluj-Napoca, Romania, between February 2023 and September 2024. Individuals were eligible if a clinical and dermatoscopic assessment suggested the presence of skin cancer. Patients with a prior history of malignancy were excluded from the study. All examinations were performed by dermatologists with more than ten years of clinical experience. Peripheral blood was collected from each participant, and serum was prepared following the laboratory's standard procedures. Ethical approval was obtained from the Iuliu Haţieganu University of Medicine and Pharmacy Cluj-Napoca (approval no. 44/31.03.2023) and the County Emergency Clinical Hospital Cluj-Napoca (approval no. 31186/5.07.2023). Written informed consent was collected from all participants. Excised tumors were processed as formalin-fixed, paraffin-embedded tissues and evaluated histologically with hematoxylin and eosin staining. A pathologist documented tumor size, histologic subtype, and grade when applicable, and only lesions confirmed as BCC were included in the subsequent analysis. The risk classification was based on the NCCN guidelines [5].

Metabolites were extracted by mixing 0.25 mL of serum with 1 mL of a methanol–acetonitrile solution (2:1, v/v). After vortexing for 30 seconds, samples were stored at −20 °C for 24 hours, then thawed and centrifuged at 12,500 g for 10 minutes. Supernatants were filtered through 0.2-µm nylon membranes and transferred into autosampler vials for analysis.

Metabolomic profiling was performed using a quadrupole time-of-flight mass spectrometer (MaXis

Impact) coupled to a liquid chromatography system (UltiMate 3000). Chromatographic separation employed a reversed-phase C18 column (Acclaim UPLC C18). The mobile phases consisted of 0.1% formic acid in water (A) and 0.1% formic acid in acetonitrile (B). A 15-minute gradient was applied at a flow rate of 0.8 mL/min, with a 5-µL injection volume and a column temperature of 28 °C. The gradient progressed from 90% to 85% A (0–3 min), 85% to 50% A (3–6 min), 50% to 30% A (6–8 min), 30% to 10% A (8–12 min), followed by re-equilibration to 90% A. Mass spectra were collected between 50 and 1000 Da. The internal standard was a 0.5 mg/mL doxorubicin hydrochloride solution (parent ion m/z= 544.1360). In parallel QC samples were analyzed for reproducibility. All measurements were done in duplicate. Mass spectra were collected from m/z 50 to 1000, enabling detection of both polar (<380 Da) and hydrophobic (>380 Da) metabolites. Nebulizer pressure was set to 2.8 bar, with a drying gas flow of 12 L/min at 300 °C. Sodium formate was used for calibration prior to each run.

Raw LC–MS data were processed with DataAnalysis v4.2, including chromatogram alignment, conversion to base-peak chromatograms, and feature detection using the Find Molecular Features algorithm. Features with retention times below 0.3 minutes, signal intensities under 3000 units, signal-to-noise ratios below 3, or m/z values above 600 Da were excluded. Alignment of m/z features was performed using the NEAPOLIS platform (https://www.bioinformatics.org/bioinfo-af-cnr/NEAPOLIS/).

Statistical analysis was carried out in R (version 4.4.2) with the objective of identifying a concise panel of metabolites associated with HR lesions, thereby generating hypotheses regarding the potential feasibility of metabolomic approaches for risk stratification in BCC. Samples were included only if at least 70% of metabolite intensities were present, and metabolites were retained if missing values did not exceed 30% across samples. Intensities were log-transformed and autoscaled. Metabolites differing between HR and LR samples were identified using two-tailed Student's t-tests. Significance required $P < 0.01$ and an absolute fold change greater than 1.2. Given the exploratory nature of the analysis, no adjustment for multiple testing was applied, as the goal was to rank metabolites according to their ability to discriminate between HR and LR lesions. The numerical imbalance between groups was not corrected for, as it arose from the consecutive inclusion of patients. Global variability was examined via principal component analysis (PCA) using prcomp() function from the stats v. 4.4.2 package, after median imputation of missing values and standardization to unit variance.

To evaluate discriminative performance, linear discriminant analysis was applied to PCA scores derived from significant metabolites. Linear discriminant analysis was performed with the MASS package (version 7.3-61), using the smallest number of principal components accounting for at least 80% of cumulative variance. Posterior probabilities generated by the model were used to assign HR vs LR classifications. Given the limited sample size, leave-one-out cross-validation was used, as external validation in an independent hold-out cohort was not feasible. Confusion matrices were derived from cross-validated predictions, and ROC curves with corresponding AUC values were computed using the pROC package (version 1.19.0.1). To generate hypotheses concerning the molecular origin of the observed metabolomic changes, pathway enrichment analysis was carried out in MetaboAnalyst 6.0 using the SMPDB reference library.

Results

Out of the 48 patients included in the study, 38 lesions were HR BCC, while 10 proved to be LR BCC. The subgroup analysis of tumor dimension, location and histologic type is depicted in Table I.

Table I. Distribution of patients classified as high-risk and low-risk basal cell carcinoma (BCC) according to NCCN criteria with subgroup analysis of risk considering tumor dimension, tumor location and histologic subtype.

	Low risk BCC	High risk BCC
NCCN guideline	10	38
Dimension (>2cm)	9	38
Location	12	35
Histology	40	8

In regard to the first aim, we were interested in delineating the metabolomic profile of HR BCC. After retaining only metabolites detected in at least 70% of samples, the dataset comprised 99 polar and 54 lipophilic compounds (Figure 1A). Using the defined significance thresholds (Student's t-test $P < 0.01$ and absolute fold change > 1.2), the volcano plot revealed 10 metabolites that differed significantly between HR and LR BCC (Figure 1B and table II).

Table II. The 10 discriminatory metabolites grouped as polar or lipophilic compounds.

Compound	Classification
Dihydroxybutyric acid	Polar
Tetradecanoylcarnitine	Polar
Adenosine monophosphate	Polar
Androsterone	Lipophilic
Deoxycholic acid	Lipophilic
Glucosylsphingosine	Lipophilic
Lysophosphatidylcholine (18:3)	Lipophilic
Lysophosphatidylcholine (18:1)	Lipophilic
Lysophosphatidylcholine (20:4)	Lipophilic
Lysophosphatidylcholine (22:5)	Lipophilic

Next, PCA was performed using only the metabolites that were significantly different in the volcano plot. The PCA score plot in figure 1C shows the distribution of samples along principal component 2 and 3. The two risk groups occupy overlapping but partially distinct areas of the plot. The separation was primarily influenced by principal component 2, which showed strong positive loadings for dihydroxybutyric acid and negative loadings for glucosylsphingosine. Principal component 3 was mainly shaped by positive contributions from androsterone and lysophosphatidylcholine (20:4), whereas lysophosphatidylcholine (22:5), lysophosphatidylcholine (18:3), and adenosine monophosphate contributed negatively.

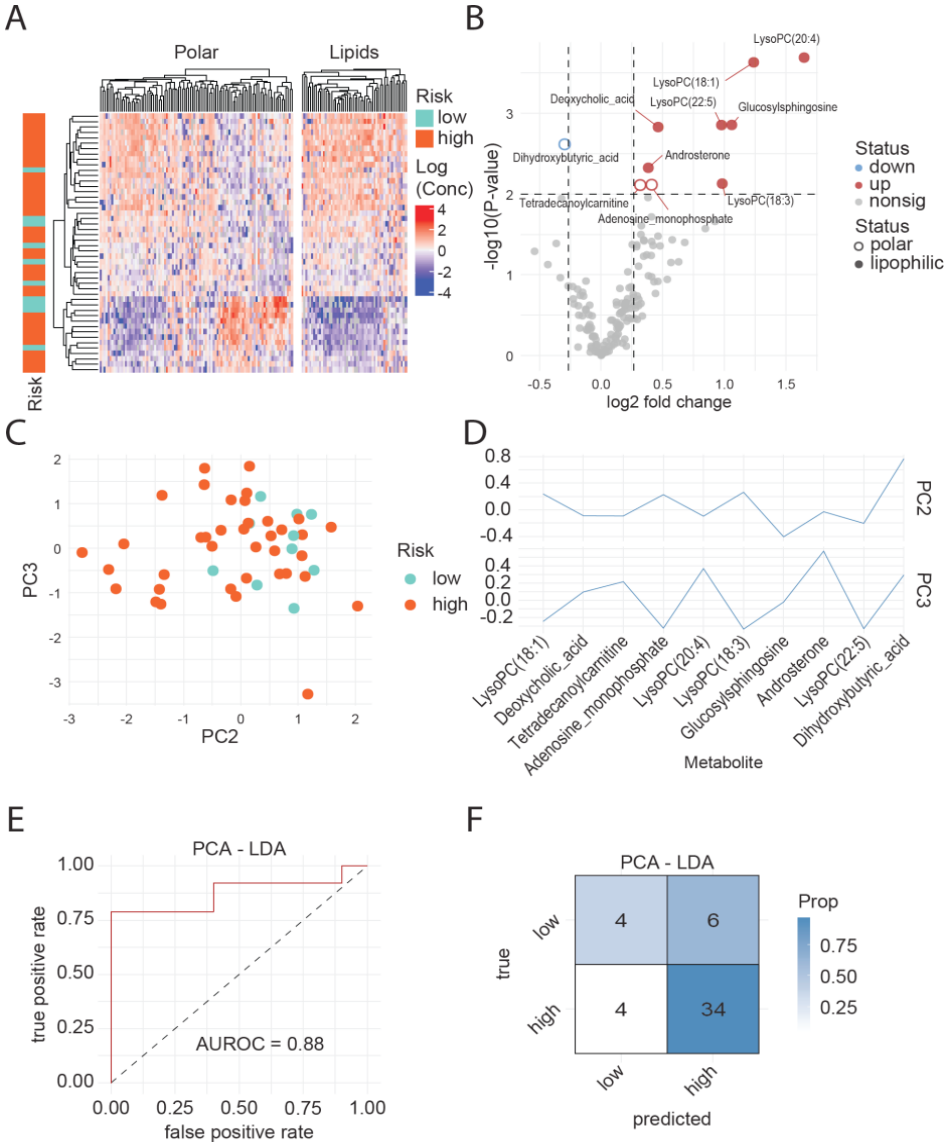

Figure 1. Serum metabolomic differences between low-risk and high-risk basal cell carcinoma.
(A) Heatmap of polar metabolites and lipid species across low-risk and high-risk samples, shown as log-transformed intensities with hierarchical clustering of both metabolites and samples.
(B) Volcano plot displaying fold changes and significance values for all detected metabolites. Features that passed the significance threshold are highlighted.
(C) PCA score plot based on significantly different metabolites, showing sample distribution along PC2 and PC3.
(D) Loading plot indicating the metabolites that contributed most to principal component 2 (PC2) and PC3.
(E) ROC curve for the principal component analysis coupled with linear discriminant analysis (PCA-LDA) classification model constructed from the significantly different metabolites.
(F) Confusion matrix for the PCA-LDA model, showing predicted and true classifications for low-risk and high-risk cases.

We used the first four principal components, which together accounted for more than 80% of the total variance in the dataset, as input for a linear discriminant analysis model. The model yielded an AUC of 0.88 (Figure 1E), while the confusion matrix corresponded to a sensitivity of 89% and a specificity of 40% in detecting HR BCC (Figure 1F).

After defining the metabolic differences between LR and HR lesions, we proceeded to perform an exploratory pathway enrichment analysis and to determine whether clinical variables such as tumor size, anatomical location, or histologic subtype contributed to the observed patterns. The enrichment analysis using the SMPDB library indicated that the selected metabolites span several chemical classes, including carboxylic acids and their derivatives, steroids and steroid derivatives, glycerophospholipids, indole compounds, diazines, and various organooxygen metabolites (Figure 1A, B).

To determine which clinical features contributed to the observed metabolic differences, we next evaluated the relationship between the discriminant metabolites and tumor size, anatomical location, and histologic subtype. No meaningful differences were observed across histologic risk classes (Figure 2C). In contrast, several metabolites differed significantly between lesions arising in HR and LR anatomical sites. Tumor size also showed a notable influence, indicating that lesion dimension is associated with distinct metabolic profiles.

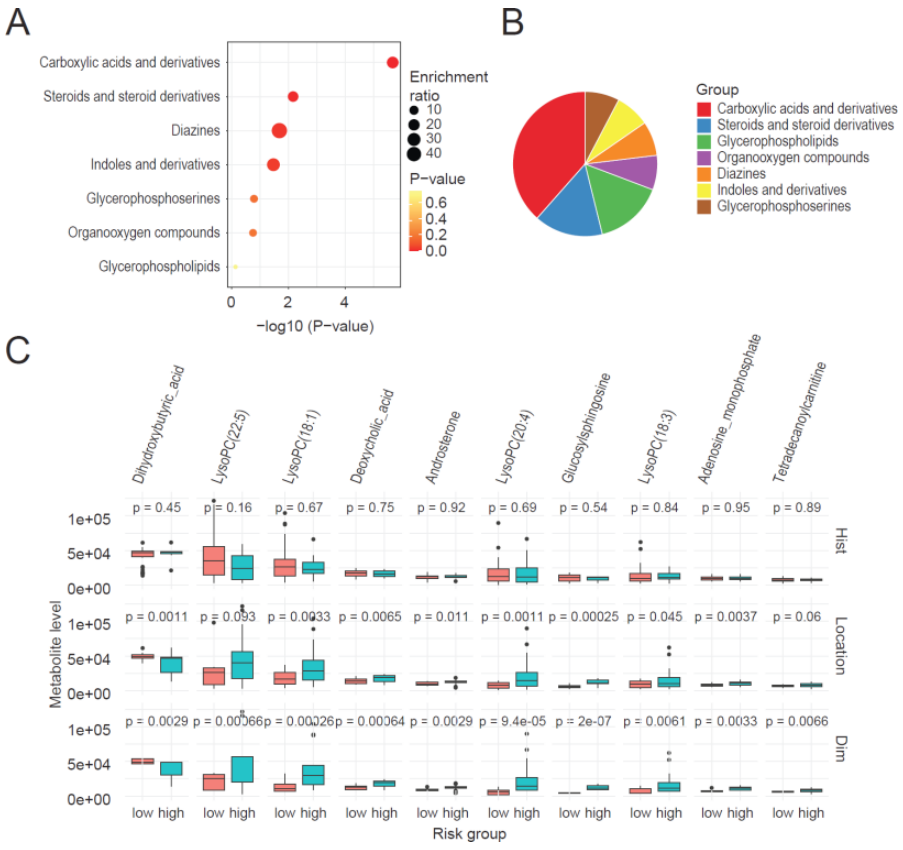

Figure 2. Functional classification of differential metabolites and their associations with tumor features.
(A) Enrichment analysis of the chemical classes represented by the differential metabolites.
(B) Proportional distribution of these metabolites across major chemical categories.
(C) Boxplots showing metabolite levels in relation to histologic subtype, anatomical location and tumor dimension. P-values for each comparison are shown above the corresponding panels.

Discussion

This study addressed two main objectives. First, we evaluated whether LR and HR BCC differ in their circulating metabolic profiles. Second, after identifying discriminant metabolites, we examined their biological relevance and assessed whether tumor size, anatomical location, or histologic subtype contributed to the observed variation.

Regarding the first objective, the results demonstrate clear metabolic differences between LR and HR BCC. After filtering, the dataset contained 99 polar and 54 lipophilic metabolites, of which 10 met the predefined significance thresholds ($P < 0.01$ and absolute fold change > 1.2). These metabolites span multiple biochemical classes, indicating broad metabolic differences between LR and HR BCC rather than a single pathway shift. The linear discriminant analysis model based on the first 4 principal components reached an AUC of 0.88, with a sensitivity of 89% and a specificity of 40% for detecting HR BCC, supporting the discriminatory potential of these metabolic features.

For the second objective, we used enrichment analysis to explore the origin of the observed metabolomic differences between HR and LR BCC. The results showed that the discriminant metabolites represented several chemical categories, including carboxylic acids, steroids, glycerophospholipids, indoles, diazines, and organooxygen compounds. The relatively limited number of samples and metabolites did not allow for an in-depth analysis of metabolic pathways potentially deregulated in HR BCC, and therefore, mechanistic links between the identified metabolites and tumor aggressiveness remain speculative.

When metabolite intensities were examined across clinical variables, histologic risk classes showed no meaningful differences. In contrast, several metabolites differed significantly between lesions arising in LR versus HR anatomical sites. Tumor size also contributed to metabolic variation, with multiple metabolites showing distinct patterns between smaller and larger tumors. These findings suggest that metabolic differences between LR and HR BCC reflect both intrinsic tumor characteristics and clinically relevant contextual factors such as location and dimension.

To date, most serum metabolomics research in skin cancer has focused on melanoma rather than BCC. Several studies have evaluated metabolite-based diagnostic signatures in melanoma, including large-scale analyses that identified amino sugar–related metabolites, lipid species, and carnitine derivatives as robust discriminators between melanoma and healthy controls [9,10,12,13]. Beyond diagnosis, a recent metabolomics study in metastatic melanoma demonstrated that baseline serum metabolites can stratify patients according to overall survival under immune checkpoint inhibitor therapy, highlighting the potential of metabolomics for prognostic assessment [11]. In contrast, data on metabolomics-based risk stratification in BCC are extremely limited, and no prior study has specifically examined circulating metabolic profiles in relation to LR versus HR BCC.

Notably, several metabolite classes identified in our cohort, including lysophosphatidylcholines, steroid-related compounds, and lipid-associated metabolites, overlap with metabolic patterns previously described in tissue-based analyses of BCC [14,15]. This convergence suggests that at least part of the tumor-associated metabolic reprogramming is reflected systemically, rather than being restricted to the local tumor microenvironment. At the same time, the detection of circulating metabolites such as dihydroxybutyric acid and glucosylsphingosine highlights additional metabolic alterations that would not be captured by tissue-restricted approaches.

Compared with prior work relying on MALDI imaging or electroporation-based lipidomics, which primarily characterize local biochemical changes within tumor tissue, the present study provides complementary information by capturing systemic metabolic differences associated with clinical risk stratification [14,15]. Furthermore, unlike genetic or Mendelian randomization studies, which infer metabolic involvement indirectly [16], our approach directly measures circulating metabolites and therefore reflects real-time biochemical alterations associated with tumor behavior. Therefore, our findings expand current knowledge by providing evidence that serum metabolomics may capture clinically relevant risk distinctions in BCC. Several limitations should be considered when interpreting the findings of this study. First, the sample size was modest, particularly for the LR group, which included fewer cases than the HR group. This imbalance may have reduced the power to detect subtler metabolic differences and contributed to the partial overlap observed in PCA. Second, the study was conducted at a single clinical center, which may limit the generalizability of the metabolic patterns identified. External validation in independent cohorts with broader demographic and geographic diversity will be necessary to confirm the robustness of the findings. Third, although the untargeted LC-MS approach enabled broad detection of serum metabolites, it did not provide absolute quantification, and certain metabolite classes, such as highly hydrophobic lipids or low-abundance compounds, may be underrepresented. Finally, mechanistic associations between the identified metabolites and BCC aggressiveness remain speculative, as the relatively small number of patients and metabolites did not permit a detailed pathway enrichment analysis. Despite these constraints, the study offers initial evidence that serum metabolomics can differentiate LR from HR BCC and supports further exploration of metabolic markers for risk stratification in BCC.

Conclusion

In summary, this study shows that LR and HR BCC have distinct circulating metabolic profiles detectable by untargeted serum LC-MS. We identified 10 metabolites that differed between the two groups, and multivariate modeling produced an AUC of 0.88, indicating that serum metabolites reflect clinically relevant differences in BCC risk. The discriminant metabolites belonged to multiple biochemical classes, and their variation was influenced mainly by anatomical site and tumor size rather than histologic subtype. Although validation in larger and more diverse cohorts is required, these results provide initial evidence that serum metabolomics may complement current clinical criteria and support more accurate risk stratification in BCC.

Acknowledgments

We thank Dr. Vlad Moisoiu for his support with the statistical analysis and his valuable input during manuscript preparation.

References

1. Peris K, Fargnoli MC, Kaufmann R, Arenberger P, Bastholt L, Seguin NB, et al. European consensus-based interdisciplinary guideline for diagnosis and treatment of basal cell carcinoma-update 2023. Eur J Cancer. 2023;192:113254.
2. Wysong A, Aasi SZ, Tang JY. Update on metastatic basal cell carcinoma: a summary of published cases from 1981 through 2011. JAMA Dermatol. 2013;149:615-616.
3. Puig S, Berrocal A. Management of high-risk and advanced basal cell carcinoma. Clin Transl Oncol. 2015;17:497-503.
4. Marzuka AG, Book SE. Basal cell carcinoma: pathogenesis, epidemiology, clinical features, diagnosis, histopathology, and management. Yale J Biol Med. 2015;88:167-179.
5. Schmults CD, Blitzblau R, Aasi SZ, Alam M, Amini A, Bibee K, et al. Basal Cell Skin Cancer, Version 2.2024, NCCN Clinical Practice Guidelines in Oncology. J Natl Compr Canc Netw. 2023;21:1181-1203.
6. Paul S, Knight A. The Importance of Basal Cell Carcinoma Risk Stratification and Potential Future Pathways. JMIR Dermatol. 2023;6:e50309.
7. Krakowski AC, Hafeez F, Westheim A, Pan EY, Wilson M. Advanced basal cell carcinoma: What dermatologists need to know about diagnosis. J Am Acad Dermatol. 2022;86(6S):S1-S13.
8. Danzi F, Pacchiana R, Mafficini A, Scupoli MT, Scarpa A, Donadelli M, et al. To metabolomics and beyond: a technological portfolio to investigate cancer metabolism. Signal Transduct Target Ther. 2023;8:137.
9. Bayci AWL, Baker DA, Somerset AE, Turkoglu O, Hothem Z, Callahan RE, et al. Metabolomic identification of diagnostic serum-based biomarkers for advanced stage melanoma. Metabolomics. 2018;14:105.
10. Bollard SM, Howard J, Casalou C, Kelly BS, O'Donnell K, Fenn G, et al. Proteomic and metabolomic profiles of plasma-derived Extracellular Vesicles differentiate melanoma patients from healthy controls. Transl Oncol. 2024;50:102152.
11. Costantini S, Madonna G, Capone M, Di Gennaro E, Bagnara P, Renza F, et al. Metabolomic signatures in liquid biopsy are associated with overall survival in metastatic melanoma patients treated with immune checkpoint inhibitor therapy. J Exp Clin Cancer Res. 2025;44:119.
12. Morsy Y, Hubeli B, Turko P, Barysch M, Martínez-Gómez JM, Zamboni N, et al. The serum metabolome serves as a diagnostic biomarker and discriminates patients with melanoma from healthy individuals. Cell Rep Med. 2025;6:102283.
13. Peña-Martín J, Belén García-Ortega M, Palacios-Ferrer JL, Díaz C, Ángel García M, Boulaiz H, et al. Identification of novel biomarkers in the early diagnosis of malignant melanoma by untargeted liquid chromatography coupled to high-resolution mass spectrometry-based metabolomics: a pilot study. Br J Dermatol. 2024;190:740-750.
14. Brorsen LF, McKenzie JS, Pinto FE, Glud M, Hansen HS, Haedersdal M, et al. Metabolomic profiling and accurate diagnosis of basal cell carcinoma by MALDI imaging and machine learning. Exp Dermatol. 2024;33:e15141.
15. Louie L, Wise J, Berl A, Shir-Az O, Kravtsov V, Yakhini Z, et al. High-throughput lipidomic profiles sampled with electroporation-based biopsy differentiate healthy skin, cutaneous squamous cell carcinoma, and basal cell carcinoma. Skin Res Technol. 2024;30:e13706.
16. Yao J, Han M. Effect of the blood cells, inflammatory cytokines, antibodies, circulating metabolome, and immune cells on skin cancers: A bidirectional 2-sample Mendelian randomization study and mediation analysis. Medicine (Baltimore). 2025;104:e43233.